

ISMRM Weekend Workshop 2015

Imaging Microstructure -- Applications Elsewhere in the Body

Roger M. Bourne PhD

Discipline of Medical Radiation Sciences | Faculty of Health Sciences THE UNIVERSITY OF SYDNEY
75 East Street | Lidcombe | NSW | 2141

E roger.bourne@sydney.edu.au | W http://sydney.edu.au/health_sciences/staff/roger_bourne

Outline

1. Learning objectives
2. Overview
3. Survey of non-neural tissue microimaging studies
4. Tissue preparation
5. Microimaging protocols
6. Acknowledgement
7. References

1. Learning objectives

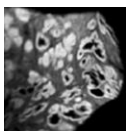
Upon completion of this course participants should be able to:

- Give an overview of MRI-based tissue microstructure studies in non-neural tissues.
- Describe methods for preparation of tissue for microimaging.
- Describe common tissue microimaging protocols.

2. Overview

This workshop contribution describes tissue microstructure imaging studies and methods for non-neural tissues. Most of the studies to date have focused on diffusion weighted imaging. Although slightly higher spatial resolution is obtained from shorter TE methods the contrast developed is generally less directly dependent on tissue structure and is thus not as useful as diffusion weighted imaging for assessment of structure variations. In this context it is noteworthy that the diagnosis and grading of many diseases, especially cancers, is primarily based on tissue microstructure assessed by light microscopy.

The structure of non-neural tissues is in general very different from and more heterogeneous than neural tissue, and the literature much less extensive. Most of the methods described here have been developed by my own research group for prostate, breast, and lymph node tissue. Due to the long imaging times



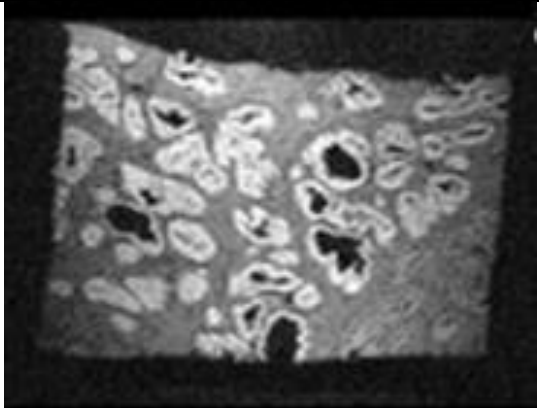
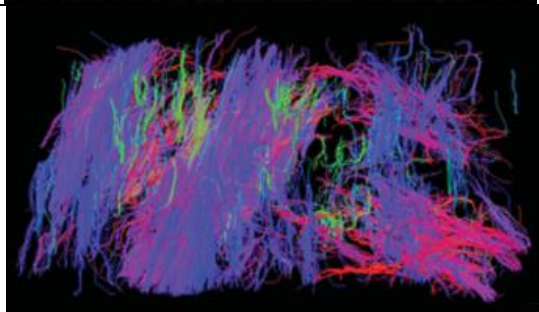
required to achieve high spatial resolution all microimaging studies to date have used formalin fixed tissue samples. In future it will be interesting to perform similar measurements in perfused unfixed samples and to carefully investigate the effects of fixation.

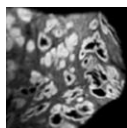
3. Survey of non-neural tissue microimaging studies

This section introduces published studies describing microimaging of non-neural tissues. It is important to note that while the tissue structures that hinder and restrict water transport in neural tissues have been intensively investigated both experimentally and theoretically, this is not the case for non-neural tissues.

3.1 Prostate

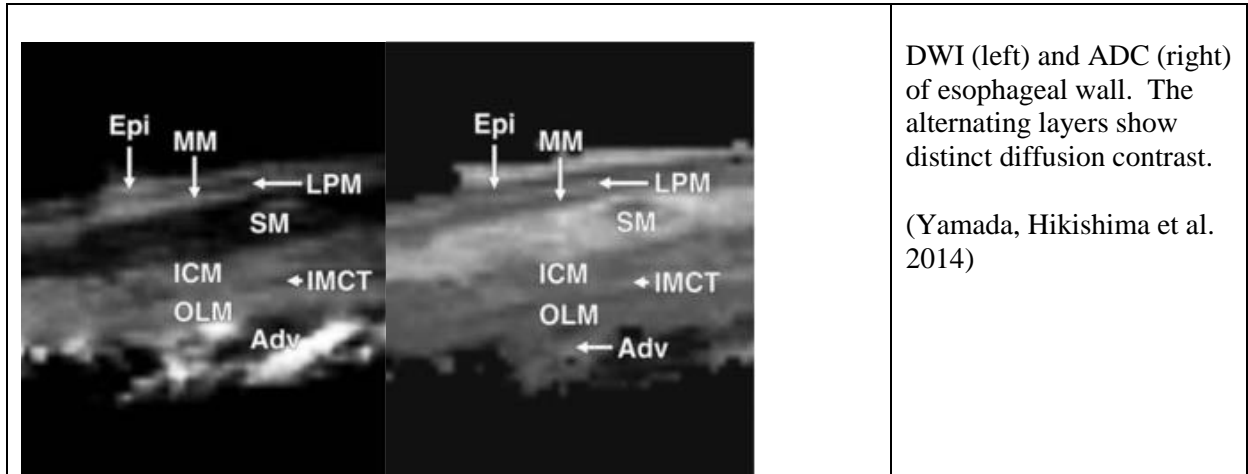
The prostate gland is comprised of a series of branching ducts lined with secretory epithelium and embedded in a fibromuscular stromal matrix. The epithelial cell layer has distinctly lower ADC than the stroma, which is in turn lower than the ADC in the lumen spaces of ducts and gland acini (Bourne, Kurniawan et al. 2010, Bourne, Kurniawan et al. 2012). The fibromuscular stromal matrix exhibits high diffusion anisotropy at very small spatial scale (40 μm isotropic voxels, (Bourne, Kurniawan et al. 2012)), however, the complex and heterogonous organization of the smooth muscle cells (and possibly the extracellular fibrous matrix), most likely leads to relatively low measured anisotropy in most voxels when performing DTI at typical clinical spatial resolution (Sinha and Sinha 2004, Gurses, Kabakci et al. 2008).

	<p>DWI of normal glandular prostate tissue showing low ADC epithelium, intermediate ADC stroma, and high ADC lumen and duct spaces (40 μm isotropic voxels). There is some T2 enhancement of the contrast. Sample is ~4 mm L-R \times 3 mm diameter.</p> <p>(Bourne, Kurniawan et al. 2012)</p>
	<p>Prostate stroma fibre tractography based on DTI measurement of normal prostate tissue (40 μm isotropic voxels). Tracts are consistent with predominant direction of myocytes.</p> <p>(Bourne, Kurniawan et al. 2012)</p>



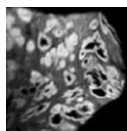
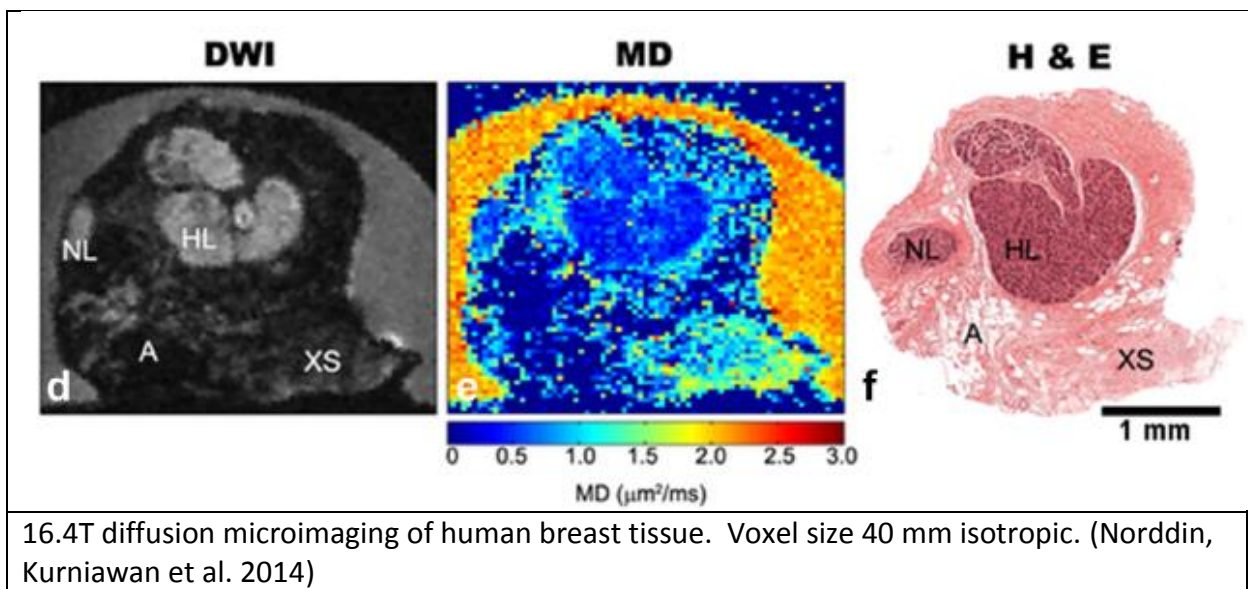
3.2 Esophagus

The esophagus has a complex structure comprising multiple layers of smooth muscle with alternating fiber orientation, layers of connective tissue, and an endothelial lining. As seen in prostate, the epithelial layer (endothelium) has a relatively low ADC.



3.3 Breast

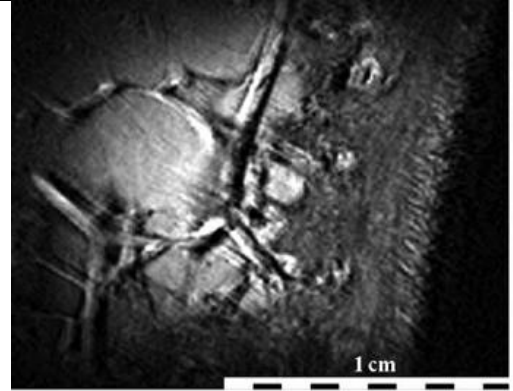
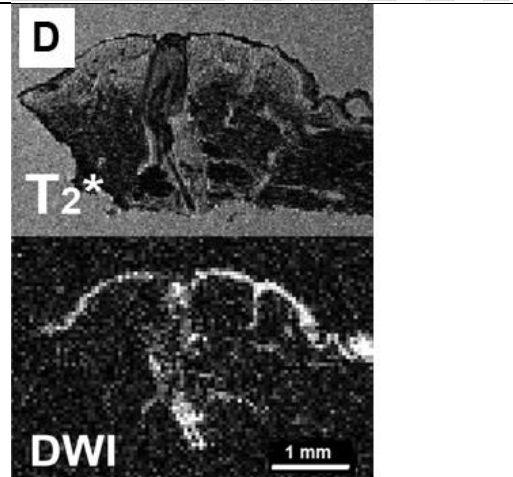
The breast gland is comprised of a series of branching ducts lined with secretory epithelium and embedded in a fatty fibrous stromal matrix. In contrast to the prostate there is no muscle tissue, but like the prostate the breast epithelia have low ADC relative to their supporting stroma (Norddin, Kurniawan et al. 2014).



The breast stroma is comprised of a collagen fiber matrix having limited orientational coherence interspersed with a heterogeneous pool of adipocytes. A microimaging study of fixed breast tissue demonstrated an increase in ADC and FA in regions of high collagen density (presumably having coherent fiber orientation) (Kakkad, Akhbardeh et al. 2013, Kakkad, Zhang et al. 2013).

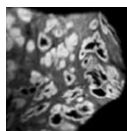
3.4 Skin

Skin has a complex multi-layered structure with numerous secondary structures including hair follicles and sweat glands. As seen in prostate, breast, and esophagus studies the epithelial layer has relatively low ADC.

	<p>T2*-weighted image of human skin in vivo at 1.5 T. Voxel size $80 \times 80 \times 80 \mu\text{m}$. The '3D' effect results from a displaced fat signal due to chemical shift artifact.</p> <p>(Laistler, Poirier-Quinot et al. 2015)</p>
	<p>16.4T T2* and DWI of formalin fixed human skin. (Bourne lab. Unpublished).</p>

3.5 Cartilage

Cartilage is made up of a dense extracellular matrix of collagen and proteoglycan. The diffusion properties have been measured at high spatial resolution (Raya, Arnoldi et al. 2011, Momot 2012). Both ADC and FA vary with cartilage zone and in some regions change under compressive load. As in breast tissue, the complex and variably disordered structure of the matrix is likely to produce complex diffusion hindrance effects while the lack of cellular structures, and in particular membranes, means restricting barriers are absent.



4. Tissue preparation

This section describes some basic techniques and considerations for preparation of non-neural tissue for microimaging.

It is advisable to plan tissue collection and processing protocols with an appropriately experienced pathologist. This is particularly important if the tissue is to be returned to the pathology department or another laboratory for histological processing.

As most microimaging studies will require tissue stabilization by formalin fixation it is desirable to plan a strategy to assess the effects of fixation. If fresh tissue is available, a reduced duration imaging protocol (possibly at low temperature) might be performed and the results compared with the same experiment performed after fixation. Tissues vary widely in rate of decomposition following devascularization and excision. Prostate, for example, shows minimal histological signs of degradation for several hours at 20°C.

Formalin fixation stabilizes tissue by crosslinking protein, leading to a general reduction in measured ADC. When a biexponential model of signal attenuation is used for prostate tissue measurements fixation produces a greater reduction of the 'slow' water pool ADC than the 'fast' pool ADC (Bourne, Bongers et al. 2013) but little change of the size of the two pools. In prostate tissue fixation decreases mean voxel FA by ~0.05 (Bourne lab. Unpublished).

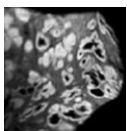
The presence of formalin drastically shortens tissue T_2 and may decrease the signal-to-noise ratio of measurements. If possible, thoroughly fixed tissue should be soaked in saline or PBS to minimize the formalin concentration prior to imaging. The time required depends on tissue type, sample size, agitation, etc.

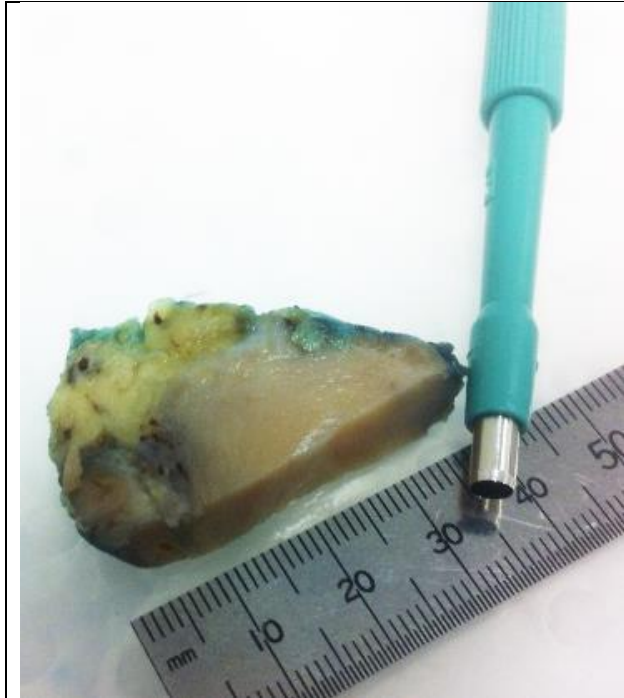
Imaging may be accelerated by selective shortening of T_1 by immersion of the sample in a paramagnetic contrast agent. We use 0.2% v/v Magnevist which gives a tissue T_1 of ~500 ms and enables use of a short TR. The possibility of selective/inhomogeneous contrast uptake/binding should be considered when interpreting observed image contrast.

Tissue samples should be degassed under vacuum prior to imaging to ensure that bubbles do not produce signal voids and susceptibility artifacts.

To reduce background signal the tissue can be immersed in perfluorocarbon liquid (eg. Fomblin). However, the perfluorocarbon may slowly infiltrate some tissues and may be difficult to wash out. An aqueous background is sometimes useful as a diffusion reference.

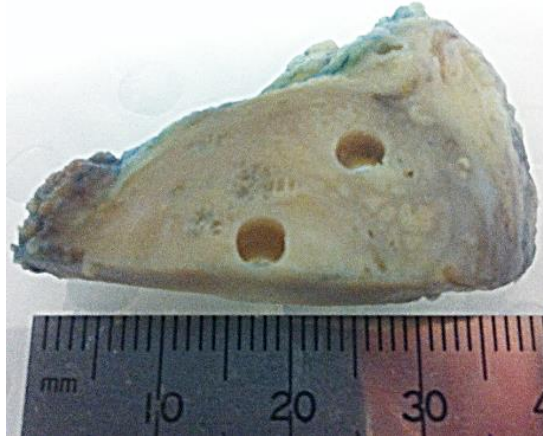
Sample mounting is important for immobilization and positioning during imaging. A solid substrate may also be useful as an orientation landmark during post-imaging tissue processing. We superglue our samples to a plastic weigh-boat and then cut the plastic according to the sample tube used for imaging.





LEFT AND BELOW: If the tissue is relatively rigid (low fat content, fixed) a neat cylinder can be cut with a biopsy punch.

eg. http://www.kai-group.com/global/en/biz/medical_dermatology_punches.html



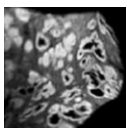
LEFT: 3-mm diameter tissue cylinders super-glued to a plastic weigh boat. The plastic is then cut to fit inside a 5-mm NMR tube. Cut plastic to position samples in center of coil.

Set imaging planes orthogonal to plastic surface.

Plastic is also useful as orientation guide for post MRI histology processing.

Weigh boat plastic dissolves in histology solvents so don't expect it to be visible in stained sections.

An insoluble base could be used but beware of damaging the microtome blade.

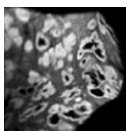


5. Imaging protocols

The following tables provide examples of the variety of instruments and techniques used for tissue microimaging.

Prostate/Breast/Lymph nodes (DWI)		
(Bourne, Kurniawan et al. 2011, Bourne, Kurniawan et al. 2012, Bourne, Kurniawan et al. 2012, Norddin, Kurniawan et al. 2014)		
Tissue prep	formalin fixation	
Sample presentation for MRI	Washed and suspended in 0.5% w/v saline + 0.2%v/v Magnevist (Dimeglumine gadopentetate 4.69 g/10 mL) in 5mm NMR tube	
B ₀	16.4 T	
Coil	5-mm solenoid or birdcage	
Voxel size	40x40x40 μm	
gradients	(Micro 2.5) 150G/cm max or (Micro 5) 300G/cm max	
directions	6	
b-values	0, 800 s/mm ²	
δ/Δ	2/12 ms	
TE/TR	30/400 ms	
Scan time	14 hr	

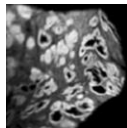
Breast (DWI)		
(Kakkad, Akhbardeh et al. 2013, Kakkad, Zhang et al. 2013)		
Tissue prep	formalin fixation	
Sample presentation for MRI	Washed in phosphate buffered saline then immersed in perfluorocarbon in 10-mm NMR tube	
B ₀	11.7 T	
Coil	10-mm 'volume coil'	
Voxel size	60x60x60 μm	
gradients	not specified	
directions	6	
b-values	0, 1500 s/mm ²	
δ/Δ, TE/TR, Scan time	not specified	



Esophagus (DWI)		
(Yamada, Hikishima et al. 2014)		
Tissue prep	formalin fixation	
Sample presentation for MRI	not described	
B ₀	7 T	
Coil	4-channel phased-array surface coil	
Voxel size	20x20x2000 μm	
gradients	700 mT/m max	
directions	1	
b-values	0 – 7163 s/mm ²	
δ/Δ	4.5/18.5 ms	
TE/TR	29/3000 ms	
Scan time	43 min	

Human Skin (T2*)		
(Laistler, Poirier-Quinot et al. 2015)		
Tissue prep	in vivo	
Sample presentation for MRI	not described	
B ₀	1.5T	
Coil	Superconducting 12mm dia. surface coil	
gradients	66 mT/m max	
Voxel size	80x80x80 μm	
TE/TR	10/38 ms	
BW	72 Hz/px	
Scan time	30 min	

Cartilage (DWI)		
(Raya, Arnoldi et al. 2011)		
Tissue prep	unfixed post mortem	
Sample presentation for MRI	Washed in phosphate buffered saline then immersed in perfluorocarbon in 10-mm NMR tube	
B ₀	17.6 T	
Coil	20-mm birdcage	
Voxel size	62x250x1000 μm	
gradients	1T/m max	
directions	6	
b-values	0, 550 s/mm ²	
δ/Δ	3/6 ms	
TE/TR	16/1000 ms	

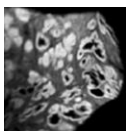


8. Acknowledgements

Some of the work described above was funded by the Australian National Health and Medical Research Council grant 1026467. I am indebted to my many hospital and university collaborators for technical assistance.

9. References

- Bourne, R., A. Bongers, N. Charles, C. Power, P. Sved and G. Watson (2013). "Effect of formalin fixation on biexponential modeling of diffusion decay in prostate tissue." Magnetic Resonance in Medicine **70**(4): 1160-1166.
- Bourne, R., N. Kurniawan, G. Cowin, P. Sved and G. Watson (2010). 16T Diffusion Tensor Microimaging of Prostate Tissue ex Vivo Demonstrates Diffusion Compartmentation Inferred from in Vivo Measurements. 96th Annual Meeting of the Radiological Society of North America. Chicago, USA, Radiological Society of North America.
- Bourne, R., N. Kurniawan, G. Cowin, P. Sved and G. Watson (2011). "16T Diffusion Microimaging of Fixed Prostate Tissue. Preliminary findings." Magnetic Resonance in Medicine **66**: 244-247.
- Bourne, R., N. Kurniawan, G. Cowin, P. Sved and G. Watson (2012). "Microscopic Diffusion Anisotropy in Formalin Fixed Prostate Tissue: Preliminary Findings." Magnetic Resonance in Medicine **68**: 1943-1948.
- Bourne, R. M., N. Kurniawan, G. Cowin, T. Stait-Gardner, P. Sved, G. Watson and W. S. Price (2012). "Microscopic diffusivity compartmentation in formalin-fixed prostate tissue." Magnetic Resonance in Medicine **68**(2): 614-620.
- Gurses, B., N. Kabakci, A. Kovanlikaya, Z. Firat, A. Bayram, A. M. Ulug and I. Kovanlikaya (2008). "Diffusion tensor imaging of the normal prostate at 3 Tesla." European Radiology **18**(4): 716-721.
- Kakkad, S., A. Akhbardeh, J. Zhang, M. Solaiyappan, D. Leibfritz, K. Glunde¹ and Z. Bhujwalla (2013). Mapping collagen 1 fiber architecture to diffusion tensor imaging in human breast tumor specimens. ISMRM 2013, Salt lake City.
- Kakkad, S., J. Zhang, Z. Bhujwalla and K. Glunde¹ (2013). Visualizing Collagen I fiber architecture in human breast tumor specimens using Diffusion Tensor Imaging. ISMRM 2013, Salt Lake City.
- Laistler, E., M. Poirier-Quinot, S. A. Lambert, R.-M. Dubuisson, O. M. Girard, E. Moser, L. Darrasse and J.-C. Ginefri (2015). "In vivo MR imaging of the human skin at subnanoliter resolution using a superconducting surface coil at 1.5 tesla." Journal of Magnetic Resonance Imaging **41**(2): 496-504.
- Momot, K. I. (2012). "Microstructural magnetic resonance imaging of articular cartilage." Biomedical Spectroscopy and Imaging **1**(1): 27-37.
- Norddin, N., N. Kurniawan, G. Cowin, L. Gluch, C. Power, G. Watson and R. M. Bourne (2014). "Microscopic diffusion properties of fixed breast tissue: Preliminary findings." Magn Reson Med: Early view (DOI 10.1002/mrm.25555).
- Raya, J., A. Arnoldi, D. Weber, L. Filidoro, O. Dietrich, S. Adam-Neumair, E. Mützel, G. Melkus, R. Putz, M. Reiser, P. Jakob and C. Glaser (2011). "Ultra-high field diffusion tensor imaging of articular cartilage correlated with histology and scanning electron microscopy." Magnetic Resonance Materials in Physics, Biology and Medicine **24**(4): 247-258.
- Sinha, S. and U. Sinha (2004). "In vivo diffusion tensor imaging of the human prostate." Magnetic Resonance in Medicine **52**(3): 530-537.



Yamada, I., K. Hikishima, N. Miyasaka, Y. Tokairin, E. Ito, T. Kawano, D. Kobayashi, Y. Eishi and H. Okano (2014). "Esophageal carcinoma: Evaluation with q-space diffusion-weighted MR imaging ex vivo." Magnetic Resonance in Medicine: Early view DOI 10.1002/mrm.25334.

Yamada, I., K. Hikishima, N. Miyasaka, Y. Tokairin, T. Kawano, E. Ito, D. Kobayashi, Y. Eishi, H. Okano and H. Shibuya (2014). "Diffusion-tensor MRI and tractography of the esophageal wall ex vivo." Journal of Magnetic Resonance Imaging **40**(3): 567-576.

